Cardinal directions for visual optic flow

M. Concetta Morrone*, David C. Burr*†, Silvia Di Pietro‡ and Maria-Antonietta Stefanelli‡

As we move through our environment, the flow of deforming images on the retinae provides a rich source of information about the three-dimensional structure of the external world and how to navigate through it. Recent evidence from psychophysical [1–4], electrophysiological [5–9] and imaging [10,11] studies suggests that there are neurons in the primate visual system – in the medial superior temporal cortex – that are specialised to respond to this type of complex 'optic flow' motion. In principle, optic flow could be encoded by a small number of neural mechanisms tuned to 'cardinal directions', including radial and circular motion [12,13]. There is little support for this idea at present, however, from either physiological [6,7] or psychophysical [14] research. We have measured the sensitivity of human subjects for detection of motion and for discrimination of motion direction over a wide and densely sampled range of complex motions. Average sensitivity was higher for inward and outward radial movement and for both directions of rotation, consistent with the existence of detectors tuned to these four types of motion. Principle component analysis revealed two clear components, one for radial stimuli (outward and inward) and the other for circular stimuli (clockwise and counter-clockwise). The results imply that the mechanisms that analyse optic flow in humans tend to be tuned to the cardinal axes of radial and rotational motion.

Addresses: *Istituto di Neurofisiologia del CNR, Via S. Zeno 51, Pisa 56127, Italy. †Dipartimento di Psicologia, Università di Firenze, Florence, Italy. ‡Dipartimento di Psicologia, Università di Roma 'la Sapienza', Rome, Italy.

Correspondence: David C. Burr
E-mail: dave@in.pi.cnr.it

Received: **7 May 1999**
Revised: **16 June 1999**
Accepted: **16 June 1999**

Published: **5 July 1999**

Current Biology 1999, 9:763–766
http://biomednet.com/elecref/0960982200900763

© Elsevier Science Ltd ISSN 0960-9822

Results and discussion

Motion detection

We first measured signal-to-noise thresholds for discrimination of various forms of coherent motion from random noise. The motion was derived from a set of 'spiral motions', with the direction of motion defined by the angle ϕ (from Equations 1 and 2, Materials and methods). In practice, this angle defines the direction in which a point is moving when it crosses the right-hand x-axis. The angle ϕ ranged from 0° to 360° in 7.5° steps; 0° refers to outward radial motion, 90° to clockwise rotation, 180° to inward radial motion and 270° to counter-clockwise rotation (Figure 1). Thresholds were measured with a two-interval forced-choice procedure, in which subjects were required to discriminate the interval in which coherent motion was displayed from another containing random noise of matched density. For each session (of about 30 trials), only one type of motion direction was displayed.

Average signal-to-noise thresholds are plotted on polar co-ordinates in Figure 1. Thresholds were slightly higher at the intermediate spiral motion directions, so the polar plot appears approximately square. This is consistent with the idea that coherent motion in all directions was detected by mechanisms tuned to the cardinal directions of radial and circular motion. The higher sensitivity for the cardinal directions is also apparent in Figure 2a, in which the same data are plotted as sensitivity (the reciprocal of the signal-to-noise threshold) on logarithmic Cartesian axes.

Factor analysis

Analysis of principal components (factor analysis) has been successfully applied to various areas of psychophysical research, such as in demonstrating the existence of mechanisms selective for spatial frequency [15–17]. This analysis attempts to explain as much of the total variance of a value as possible with as few factors, or principle components, as possible. If optic flow is computed by a small number of mechanisms, each with its own independent noise source, then the variance should be maximal when different mechanisms are stimulated, and these mechanisms should emerge as factors.

We therefore performed statistical factor analysis on the sensitivity data. Two significant factors emerged, accounting for 62% of the variance of data. Figure 2b shows the strength of these factors (after appropriate rotation) as a function of motion direction. Each factor has two clear peaks separated by about 180°: for one factor these fall at around 0° and 180°, and for the other at around 90° and 270°. This result suggests a common noise source for outward and inward radial motion, distinct from a separate common noise source for clockwise and counter-clockwise rotation, and strongly implies the existence of detectors of motion tuned to the cardinal directions of radial and circular motion.

Figure 1

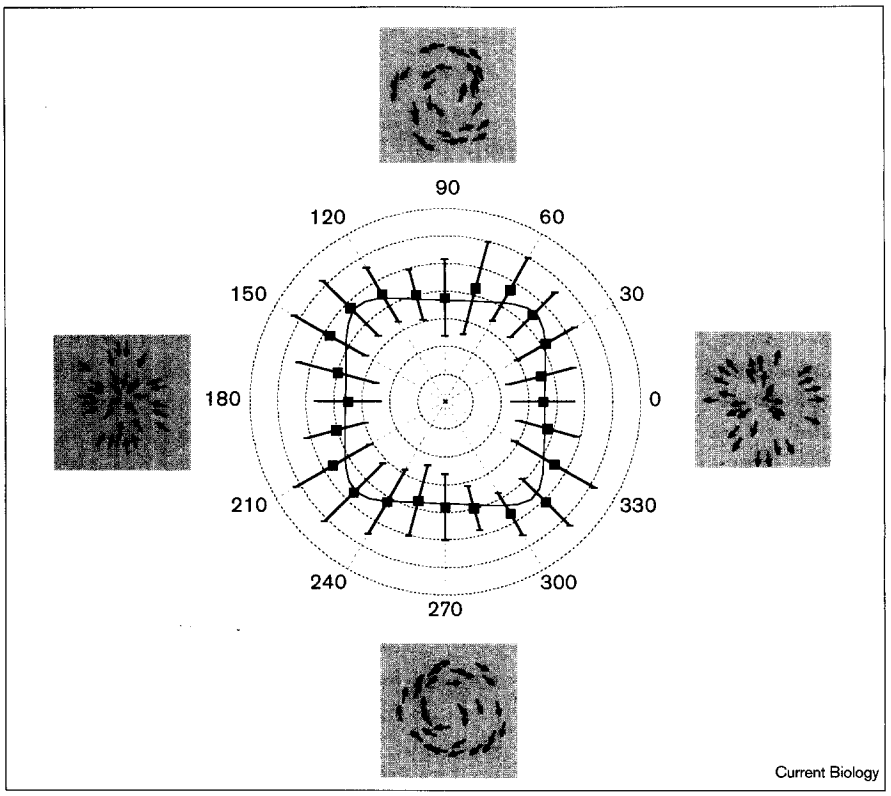

Average signal-to-noise thresholds for detecting spiral motion of various directions. The geometric mean is plotted on polar coordinates and error bars indicate average standard deviation across subjects, after removal of a general sensitivity factor. The type of motion at each of the four principle directions is illustrated. Thresholds, represented by the distance from origin, refer to the minimum ratio of signal (coherently moving dots) to noise (randomly moving dots) necessary to detect the coherent motion from randomly moving dots of matched density. The polar scale is divided in units of 0.1. The data show that the thresholds for radial and circular motion were lower than those for the other spiral motions. All forms of spiral motion can be decomposed into radial and circular motion; in this representation, the amount of the radial and circular component is given by the projection onto the x and y axes. The fact that the data tend to follow an approximately square shape suggests that for all types of spiral motion, either the radial or the circular component of that motion must reach its independent threshold, suggesting the existence of mechanisms tuned to these types of motion. The smooth curve passing through these points was the best fit of the sensitivity data to Equation 4 (see Materials and methods), replotted as thresholds.

Any form of spiral motion can be decomposed into component vectors of radial and circular motion. If detectors tuned to these motions exist, and if they act independently, they should each respond to the vector component of this motion contained in each form of spiral motion. This component is given by a rectified cosinusoidal function centred on the cardinal axes. We therefore fitted the factor strengths with rectified cosine waveforms that were free to vary in both phase and amplitude (Equation 3, Materials and methods). The fit (shown by the smooth curves in all figures) adequately describes most of the variation in the data. The phases of the fit were 12° and 90° (± 5°), suggesting that the peak sensitivity of putative neural mechanisms occurs at those motion directions, as well as at the reverse directions of 192° and 270°.

The factor strengths describe correlations between the data, without directly predicting sensitivity. Sensitivity can be estimated from the action of independent mechanisms tuned to these motion directions, however, by combining their output by the standard procedure of 'probability summation' (Equation 4, Materials and methods). The fit, shown in both Figure 1 and Figure 2a produced estimates of roughly equal weights for the two factors and suggested that there was very little interaction between them.

Motion discrimination

We also measured signal-to-noise sensitivity for discriminating the direction of spiral motion. In a given session, stimuli moved in one of two opposite directions, and subjects had to identify the direction: outward from inward radial motion , clockwise from counter-clockwise rotation, and so on. For this experiment, ϕ was restricted to the range of 0° to 90° (and thus also 180° to 270°). Average signal-to-noise sensitivity is plotted in Figure 3a on logarithmic Cartesian co-ordinates. In this set of measurements, sensitivity for radial motion was slightly higher than for circular motion, a finding that was not apparent in the motion detection data. There was also a slightly higher sensitivity for the cardinal directions, and, although this was not very obvious in the averaged data, being partly obscured by the higher sensitivity for radial motion, it was more obvious in the data for single subjects (data not shown). Factor analysis of the direction discrimination data also revealed two major components, centred around 8° and 81° (± 3°), explaining more than 88% of the variance. The factor strengths, together with their cosine fit, are shown in Figure 3b.

Given the problem of unequal sensitivity in this motion direction discrimination task, it was not meaningful to fit averaged data with the factor strengths of the component

Figure 2

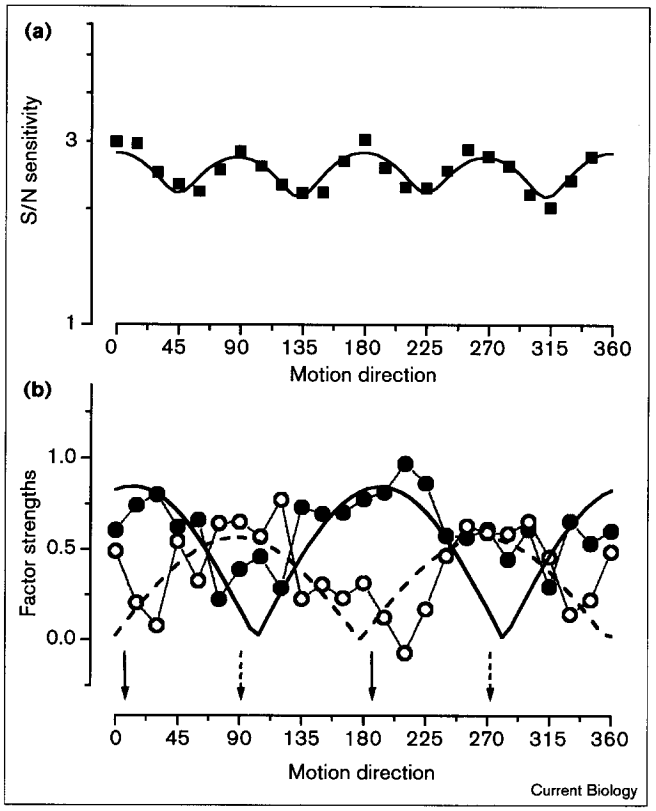

Sensitivity for detecting spiral motion, and the factors underlying this detection. **(a)** The data of Figure 1, replotted as signal-to-noise (S/N) sensitivity (the reciprocal of thresholds) on logarithmic Cartesian coordinates. The smooth curve is the fit from Equation 4 ($c_1 = 2.7$, $c_2 = 2.5$, $\beta = 6.0$). **(b)** Strengths of the two principal factors for each stimulus direction are plotted against motion direction (see Materials and methods). Filled circles and solid lines and arrows refer to the first factor; open circles and dotted lines and arrows refer to the second factor. The smooth curves are cosinusoidal fits to these factor strengths (Equation 3), with phase and amplitude free to vary. The arrows on the x axis indicate the phases of the fits (12° and 192°, and 90° and 270°).

Figure 3

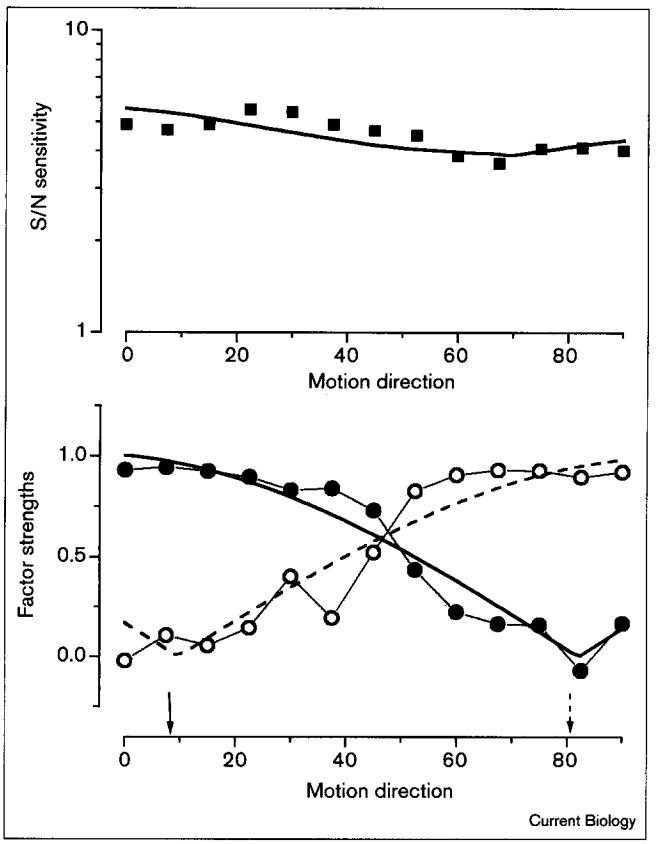

Sensitivity for discriminating the direction of spiral motion, and the factors underlying this discrimination. **(a)** A logarithmic Cartesian plot of geometric mean signal-to-noise (S/N) sensitivity for discriminating the direction of motion, as a function of motion direction. **(b)** The strengths of the two components of the factor analysis for each direction of motion. Filled circles and solid lines and arrows refer to the first factor; open circles and dotted lines and arrows refer to the second factor. As in Figure 2b, the smooth curves are cosinusoidal fits to these factor strengths. The phases of the fits are 8° and 81° (arrows).

vectors, as we did with the motion detection task. We therefore fitted individual data separately, then averaged the results of the fit (shown by the smooth curve of Figure 3a). The average of the fit is not as striking as for the detection data, but adequate. The individual fits were all satisfactory, indicating independence of the two factors from each other.

Both the sensitivity data and the factor analysis point strongly towards the existence of cardinal axes for optic flow motion that are tuned to radial and circular directions. At first sight, the results may seem to be inconsistent with the electrophysiological reports of neurons tuned to the intermediate directions of motion [6,7]. There could be several reasons for this discrepancy, including species-specific differences. Alternatively, motion detectors tuned to all motion directions may be present in humans, but the intermediate detectors may be less sensitive, so those tuned to the cardinal directions dominate the sensitivity measurements. Our results are also inconsistent with some evidence for spiral detectors in humans from psychophysical studies, which use entirely different techniques (adaptation) [14]. It is possible, however, that these studies do not investigate the operation of high-level detectors specialised for the analysis of optic flow. Rather, they may operate at a relatively low level, on local-motion mechanisms that provide input to the higher-level analysers. There is evidence from a recent study in our laboratory, using a masking paradigm, suggests that this may be so [18].

Materials and methods

Stimuli

The stimuli comprised 360 randomly positioned dots that moved in coherent motion. The motion is most easily defined as the framewise

increment in the polar co-ordinates r and θ (radius and angle) of each randomly positioned dot:

$$\Delta r = v\cos(2\pi\phi) \quad (1)$$
$$\Delta\theta = v\sin(2\pi\phi)/r \quad (2)$$

In these equations, v is local speed (4°/sec) and the angle ϕ defines the direction of the flow motion: 0 and π (0° and 180°) specify outward and inward radial motion, 90° and −90° specify clockwise and counter-clockwise rotation; all other angles specify intermediate spiral motions. Note that the angular velocity is not constant, but normalised by the radius to produce constant local speed of all elements.

The dots, which were half black, half white, 1.5 min of arc in diameter, and of 100% contrast, were displayed on a 10° square grey screen of mean luminance 50 cd/m^2. Their motion had a 'limited lifetime' of two motion frames: after each dot moved, it was extinguished, to be 'reborn' in a new random position [19]. The frame-rate of the motion display was 20 Hz (50 msec per position). The display monitor ran at 120 Hz frame-rate, updated every six frames. The display was temporally curtailed within a Gaussian window of $\sigma = 50$ msec.

Subjects were tested on two separate tasks: motion detection and discrimination of motion direction. For detection, the subjects were required to identify the temporal interval containing coherent motion (from a two-interval presentation in which the other interval had random noise of matched density). For direction discrimination, they were required to discriminate the direction of motion from its opposite in a one-interval presentation. On a given session of 30 trials, the direction of motion was always the same, and known to the subject. All subjects performed five 30-trial sessions for detection and five for direction discrimination, the first of which was discarded. The data from the others were plotted as probability-of-seeing curves, to which a cumulative Gaussian curve was fitted to measure threshold. For the detection, 14 subjects were used, and for the discrimination task, 12 were used, all 23–26 years of age and with normal or corrected vision.

Factor analysis and curve fitting

The data were factor-analysed using the Microsoft program *Statistica*. For both sets of data, a single factor did not account significantly for all the variance (53% and 51% for detection and discrimination, respectively; chi-square test $P\chi(\chi^2,\nu)$: detection $P\chi(245,252) > 0.61$; discrimination $P\chi(183,65) > 0.999$). Adding a second factor reduced the residual variance so it was not significantly different from zero; for detection, this factor accounted for 38% of the variance, and the probability that the residual variance was zero was given by $P\chi(188,229) < 0.02$; for discrimination, the factor accounted for 12% and $P\chi(27,53) < 0.002$. Adding a third factor did not significantly reduce further the residual variance (34% for detection, 10% discrimination, $p > 0.5$ (reduced chi-square test)). The factors were rotated using the 'biquartimax' method, which maximises variability between subjects and along stimulus dimensions. We also performed factor analysis on partial data, sampled over both subjects and stimulus type (similar to the bootstrap technique [20]), and found that the emerging factors were quite robust.

Factor loadings were fitted to rectified cosine waveforms:

$$F_i(\phi) = a_i\,|\cos(\phi + \phi_i)\,| \quad (3)$$

where F_i is the individual factor and ϕ is the stimulus angle (Equations 1 and 2). The amplitudes a_i and phases ϕ_i were free to vary, and were estimated by least-squares fit (simplex method). These equations were used to fit the sensitivity data in log units (S), following the standard procedure of probability summation:

$$S_\phi = \left(c_1|\cos(\phi+\phi_1)|^\beta + c_2|\cos(\phi+\phi_2)|^\beta\right)^{1/\beta} \quad (4)$$

The value of β for the fits of Figures 1 and 2a was 6.0. For the individual fits of the discrimination data, the value of β ranged from 2.5 to 5.

References

1. Regan D, Beverly KI: **Looming detectors in the human visual pathway.** *Vision Res* 1978, **18**:415-421.
2. Morrone MC, Burr DC, Vaina L: **Two stages of visual processing for radial and circular motion.** *Nature* 1995, **376**:507-509.
3. Burr DC, Morrone MC, Vaina L: **Large receptive fields for optic flow direction in humans.** *Vision Res* 1998, **38**:1731-1743.
4. Snowden RJ, Milne AB: **Phantom motion aftereffects – evidence of detectors for the analysis of optic flow.** *Curr Biol* 1997, **7**:717-722.
5. Tanaka K, Saito H: **Analysis of motion of the visual field by direction, expansion/contraction and rotation cells clustered in the dorsal part of the MST area of the macaque monkey.** *J Neurophysiol* 1989, **62**:626-641.
6. Duffy CJ, Wurtz RH: **Sensitivity of MST neurons to optic flow stimuli. I. A continuum of response selectivity to large field stimuli.** *J Neurophys* 1991, **65**:1329-1345.
7. Graziano MSA, Andersen RA, Snowden RJ: **Tuning of MST neurons to spiral motions.** *J Neurosci* 1994, **14**:54-67.
8. Britten KJ, van Wezel RJ: **Electrical microstimulation of cortical area MST biases heading perception in monkeys.** *Nat Neurosci* 1998, **1**:59-63.
9. Wurtz R: **Optic flow: a brain region devoted to optic flow analysis?** *Curr Biol* 1998, **8**:R554-R556.
10. Tootel RBH, Reppas JB, Kwong KK, Malach R, Born RT, Brady TJ, *et al.*: **Functional analysis of human MT and related visual cortical areas using magnetic resonance imaging.** *J Neurosci* 1995, **15**:3215-3230.
11. Tosetti M, Montanaro M, Morrone MC, Burr DC, Fiorentini A, Cioni G: **FMRI response of human MT complex is selective to change of direction of optic flow fields.** *Neuroimage* 1999, in press.
12. Koenderink JJ: **Optic flow.** *Vision Res* 1986, **26**:161-168.
13. Verri A, Girosi F, Torre V: **Mathematical properties of the two-dimensional motion field: from singular points to motion parameters.** *J Opt Soc Am A* 1988, **6**:698-712.
14. Snowden RJ, Milne AB: **The effects of adapting to complex motions: position invariance and tuning to spiral motions.** *J Cog Neurosci* 1996, **8**:435-452.
15. Sekuler R, Wilson HR, Owsley C: **Structural modeling of spatial vision.** *Vision Res* 1984, **24**:689-700.
16. Young RA: **Principal-component analysis of macaque lateral geniculate nucleus chromatic data.** *J Opt Soc Am A* 1986, **3**:1735-1742.
17. Peterzell DH, Teller DY: **Spatial frequency tuned covariance channels for red-green and luminance modulated gratings: psychophysical data from human adults.** *Vision Res* 1999, in press.
18. Burr DC, Ross J, Badcock DR: **Cardinal directions for optic flow.** *Perception* 1999, in press.
19. Morgan MJ, Ward R: **Conditions for motion flow in dynamic visual noise.** *Vision Res* 1980, **20**:431-435.
20. Efron B, Tibshirani RJ: *An Introduction to the Bootstrap. Monographs on Statistics and Applied Probability.* Vol. 57. New York: Chapman and Hall; 1993.